Low pressure carbon dioxide solubility in pure electrolyte solvents for lithium-ion batteries as a function of temperature. Measurement and prediction

Published in:
The Journal of Chemical Thermodynamics

Queen's University Belfast - Research Portal:
Link to publication record in Queen's University Belfast Research Portal

Low pressure carbon dioxide solubility in pure electrolyte solvents for lithium-ion batteries as a function of temperature. Measurement and prediction

Mérièm Anouti [a,*], Yvon Rodrigue Dougassa [a], Cécile Tessier [b], Loubna El Ouatani [b], Johan Jacquemin [a,c,*]

[a] Université François Rabelais, Laboratoire PCMB (EA 4244), équipe Chimie-physique des Interfaces et des Milieux Electrolytiques (CIME), Parc de Grandmont, 37200 Tours, France
[b] Direction de la Recherche – SAFT, SAFT, 33000 Bordeaux, France
[c] CenTACat, School of Chemistry and Chemical Engineering, Queen's University Belfast, Belfast BT9 5AG, Northern Ireland, UK

ARTICLE INFO

ABSTRACT

Experimental values for the carbon dioxide solubility in eight pure electrolyte solvents for lithium ion batteries – such as ethylene carbonate (EC), propylene carbonate (PC), dimethyl carbonate (DMC), ethyl methyl carbonate (EMC), diethyl carbonate (DEC), γ-butyrolactone (γBL), ethyl acetate (EA) and methyl propionate (MP) – are reported as a function of temperature from (283 to 353) K and atmospheric pressure. Based on experimental solubility data, the Henry's law constant of the carbon dioxide in these solvents was then deduced and compared with reported values from the literature, as well as with those predicted by using COSMO-RS methodology within COSMOthermX software and those calculated by the Peng–Robinson equation of state implemented into Aspen plus. From this work, it appears that the CO_2 solubility is higher in linear carbonates (such as DMC, EMC, DEC) than in cyclic ones (EC, PC, γBL). Furthermore, the highest CO_2 solubility was obtained in MP and EA solvents, which are comparable to the solubility values reported in classical ionic liquids. The precision and accuracy of the experimental values, considered as the per cent of the relative average absolute deviations of the Henry's law constants from appropriate smoothing equations and from literature values, are close to (1% and 15%), respectively. From the variation of the Henry's law constants with temperature, the partial molar thermodynamic functions of dissolution such as the standard Gibbs free energy, the enthalpy, and the entropy are calculated, as well as the mixing enthalpy of the solvent with CO_2 in its hypothetical liquid state.

© 2012 Elsevier Ltd. All rights reserved.

1. Introduction

Since the beginning of the industrial revolution, human activity has been based on non-renewable fossil fuels. This induces economical and political problems. Additionally, in the light of the relationship between climate change and the increase of carbon dioxide concentration in the atmosphere, environmental problems such as global warming caused by the human activity have come to the fore [1]. One way to limit the formation of carbon dioxide in the atmosphere and to reduce emissions from vehicles has been the development of electric vehicles (EVs), which are mainly based on the lithium-ion battery technology [2]. In fact, the lithium ion battery is the most competitive power source for electric vehicles needed in the future, thus attracting extensive interest [3–6]. The four primary functional components of a lithium-ion battery are the separator, anode, cathode, and electrolyte. Commercial lithium-ion batteries contain generally liquid electrolytes based on a lithium salt dissolved in a specific solvents mixture [7,8]. Currently, the most suitable solvents for lithium ion battery remain cyclic alkyl carbonates, such as propylene carbonate (PC) and ethylene carbonate (EC), and linear alkyl carbonates, such as dimethyl carbonate (DMC), ethyl methyl carbonate (EMC) and diethyl carbonate (DEC). Other solvents like ester such as ethyl acetate (EA), methylpropanoate (MP) and γ-butyrolactone (γ-BL) are also generally used due to their low melting points, which provide better performances of the electrolyte under low temperature [9,10]. Nevertheless, the performance of a lithium ion battery depends to a great extent on the stability of electrolyte solution, because the high voltage of the battery may cause the decomposition of lithium salt or organic solvents [11–13].

During the battery charging process, the electrolyte is reduced and oxidised at the negative and positive electrodes, respectively. As already documented by several authors, such a process induces decomposition of the electrolyte, limiting the battery lifetime [14,15]. For example, when a high potential is applied to the electrode, the oxidation of the electrolyte leads to the formation of carbon dioxide, which increases the pressure inside the sealed cell [15–17]. Furthermore, the carbon dioxide formation also changes

* Corresponding authors. Address: Université François Rabelais, Laboratoire PCMB (EA 4244), équipe Chimie-physique des Interfaces et des Milieux Electrolytiques (CIME), Parc de Grandmont, 37200 Tours, France (J. Jacquemin).
E-mail addresses: meriem.anouti@univ-tours.fr (M. Anouti), johan.jacquemin@qub.ac.uk (J. Jacquemin).

the composition of the electrolyte driven by the solubility of the carbon dioxide in this solution. These effects caused by the formation of the carbon dioxide can be evaluated with the prior knowledge of the CO_2 solubility in pure electrolyte solvents.

In the present paper, the solubility of carbon dioxide in eight pure electrolyte solvents for lithium ion batteries – such as ethylene carbonate (EC), propylene carbonate (PC), dimethyl carbonate (DMC), ethyl methyl carbonate (EMC), diethyl carbonate (DEC), γ-butyrolactone (γBL), ethyl acetate (EA) and methyl propionate (MP) – are reported as a function of temperature from (283 to 353) K and atmospheric pressure. An experimental procedure based on chemical titration methodology has been used during this work. These selections of solvents and experimental techniques were chosen first to confirm previous data published by our group [18], and to evaluate these data with those already published by other groups [19–33]. Secondly, an attempt was made to estimate from the solubility data as a function of temperature the Henry's law constants and dissolution properties like the Gibbs energy, the standard enthalpy and entropy of dissolution, as well as the mixing enthalpy of the solvent with CO_2 in its hypothetical liquid state. Thirdly, we have tried to cover different families of solvents that could best illustrate solvent effects on the CO_2 solubility like the size of the molecule (DMC versus EMC versus DEC) or its basic structure (linear versus cyclic), which can drive different dissolution pathways. Furthermore, based on their relatively low vapour pressure and their cost, these solvents are sometimes referred to as a "green adsorbents" for CO_2 capture which present high CO_2 solubility in comparison with molecular solvents, like water or alcohols [23,30,34]. In order to analyse their CO_2 capture capability in greater detail, a comparison has been realised between CO_2 solubility data presented herein with those reported for another family of designer solvents like ionic liquids [35]. Additionally, this comparison was realised since ionic liquids are generally used as additive in electrolyte for lithium-ion battery applications [36]. Finally, the CO_2 solubility in these eight solvents has been calculated by the COSMO-RS methodology, and the Peng–Robinson equation of state by using directly two chemical engineering software programmes like COSMOthermX and Aspen 2006 plus, respectively. These calculated values are then compared with experimental results to evaluate the predictive capability of the CO_2 solubility in pure-electrolyte solvents of both methods.

2. Experimental

2.1. Materials

Highly pure (GC grade, mole fraction purity > 0.9999) cyclic carbonates (propylene carbonate (PC), ethylene carbonate (EC)), linear carbonates (dimethylcarbonate (DMC), ethyl methyl carbonate (EMC), and diethyl carbonate (DEC)), γ-butyrolactone (γBL), ethyl acetate (EA) and methyl propionate (MP) were obtained from Aldrich and were used as received. NaOH ($0.5 \, mol \cdot dm^{-3}$) and HCl ($1 \, mol \cdot dm^{-3}$) solutions, used to determine the amount of CO_2 dissolved in solvents using the chemical titration methodology, were obtained from Sigma Aldrich (Riedel-de Haen). The HCl ($0.2 \, mol \cdot dm^{-3}$) solutions prepared with double distilled water were standardised the NaOH commercial solution using potentiometric titration. Prior any solubility measurement, solvents are analysed for water content using coulometric Karl-Fischer (Coulometer 831 – Metrohm) titration. The water content of selected solvents, measured after treatment, is close to $(10 \pm 1) \cdot 10^{-6}$.

The gases used (AGA/Linde Gaz) have the following specifications: carbon dioxide, mole fraction purity of 0.99995; and argon, mole fraction purity of 0.999997. All gases were used as received from the manufacturer. Information (i.e. source, abbreviation, purity, and water content) for each chemical sample studied in this paper are summarized in table 1.

2.2. Experimental method

The experimental apparatus used during the CO_2 solubility measurements reported in this present work is based on a chemical titration technique, which was already described by our group elsewhere [18], and schematically represented herein in figure 1. Under a dry atmosphere in a glove box, a known quantity of pure solvent, determined gravimetrically with an accuracy of $\pm 1 \cdot 10^{-4}$ g using a Sartorius 1602 MP balance, was first placed into equilibrium cell (EqC) equipped with a septum to avoid air and moisture contaminations during measurements. The EqC was then immersed in a water bath maintained at constant temperature, $T_{exp.}$ using a PID temperature controller and accurately measured with a calibrated $100 \, \Omega$ platinum resistance thermometer within accuracy better than ± 0.1 K. The solvent was then saturated with CO_2 at atmospheric pressure by dissolving the gas in the liquid at constant temperature for 1 h to reach the equilibrium. Different times were also examined to ensure that the saturation had been reached. When the saturation was achieved an argon flow was used to displace the amount of dissolved CO_2 in the solvent from the equilibrium cell to the titration cell, which contains a known concentration of NaOH aqueous solution. To ensure that a solvent-free (Ar + CO_2) gas mixture was introduced in the NaOH titration cell, the gas mixture was first passed through an ethanol bath at $T = 193$ K, which retains the solvent from the gas stream. The displaced quantity of dissolved CO_2 then reacts with NaOH solution by forming sodium carbonate (e.g. Na_2CO_3). The aqueous solution containing the sodium carbonate as well as the non-reacted NaOH was finally titrated by a known concentration of HCl solution, C_{HCl} as described in figure 2, where, the first and second peaks correspond to the titrations of non-reacted NaOH and sodium carbonate, respectively. The difference of volumes between these two

TABLE 1
Source, abbreviation, purity, and water content for each chemical sample reported during this work.

| Chemical name	Source	Abbreviation	Mole fraction purity	Water content 10^{-6}
Propylene carbonate	Aldrich	PC	0.9999	<10
Ethylene carbonate	Aldrich	EC	0.9999	<10
Dimethylcarbonate	Aldrich	DMC	0.9999	<10
Ethyl methyl carbonate	Aldrich	EMC	0.9999	<10
Diethyl carbonate	Aldrich	DEC	0.9999	<10
γ-Butyrolactone	Aldrich	γBL	0.9999	<10
Ethyl acetate	Aldrich	EA	0.9999	<10
Methyl propionate	Aldrich	MP	0.9999	<10
Sodium hydroxide Standard solution, $0.5 \, mol \cdot dm^{-3}$	Riedel-de Haen	NaOH	–	–
Hydrochloric acid standard solution, $1 \, mol \cdot dm^{-3}$	Riedel-de Haen	HCl	–	–
Carbon dioxide	AGA/Linde Gaz	CO_2	0.99995	–
Argon	AGA/Linde Gaz	Ar	0.999997	–
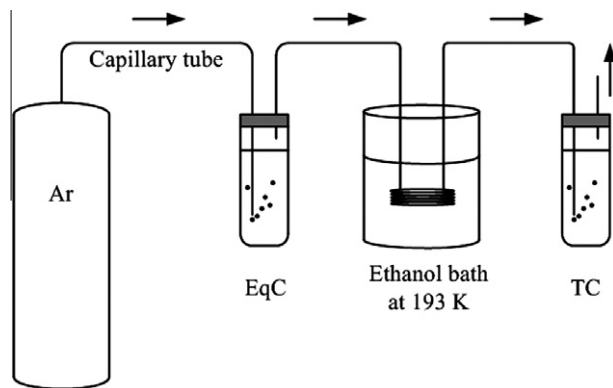
FIGURE 1. Solubility equipment used in this work: EqC, equilibrium cell containing the CO_2 saturated solvent; TC, titration cell containing the NaOH aqueous solution.
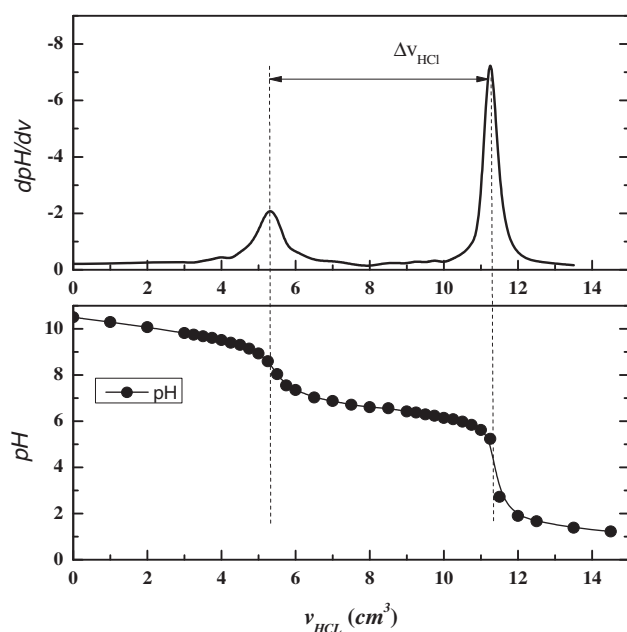

FIGURE 2. Example of the variation of the pH and its derivate with the respect to the HCl volume added as a function of the HCl volume, where ΔV_{HCl} corresponds to the HCl volume added during the titration of dissolved CO_2 in the solvent.

peaks, ΔV_{HCl}, calculated by using the derivative method of the pH with the respect to the HCl volume added, is directly link to the amount of dissolved CO_2 in the solvent, n_2:

$$n_2 = \Delta V_{HCl} \cdot C_{HCl}. \tag{1}$$

The solubility of the CO_2 in the solvent studied can be expressed in mole fraction of CO_2 in solution, x_2:

$$x_2 = \frac{n_2}{n_1 + n_2}, \tag{2}$$

where n_2 is the amount of CO_2 dissolved in the solvent and n_1 is the total amount of solvent introduced in the equilibrium cell.

Henry's law constants can be then calculated from the CO_2 mole fraction solubility as:

$$K_H = \lim_{x_2 \to 0} \frac{f_2(p, T, x_2)}{x_2} \approx \frac{\phi_2(p_{exp}, T_{exp}) p_{exp}}{x_2} \tag{3}$$

where f_2 is the fugacity of the CO_2 and ϕ_2 its fugacity coefficient calculated from the compilation of Dymond and Smith [37] at atmospheric pressure, p_{exp} and fixed temperature, T_{exp}.

The determination of the solubility at different temperatures from (283 to 353) K is simply done by changing the water bath set point and by repeating the same saturation and titration procedures. Each measurement was run in triplicate to avoid any experimental error.

2.3. Predictive methods

As proposed by Klamt et al. [38] COSMO-RS combines statistical thermodynamics methodology with the electrostatic theory of locally interacting molecular surface descriptors. These descriptors are calculated from quantum chemistry method known as COSMO (Conductor-like Screening Model). During this work, the same methodology as already presented by Ab Manan et al. [39] was used to optimise each structure and to calculate the CO_2 solubility in selected solvents, as well as in solvents containing additive salts like $LiPF_6$ or $[C_2mim][NTf_2]$ ionic liquid where each reported binary composition describes the liquid phase used in the COSMO-thermX software. As the calculation of the gas solubility by using COSMOThermX software (version 2.1, release 01.06) requires the prior knowledge of pure compound vapour pressures of pure components, these data were taken from the literature for the CO_2 [40] and also for each studied solvent [41–46]. Vapour pressures were also estimated by generating 'energy values' by using Turbomole program [47], as already described into the literature [39,48].

According to the Aspen documentation [49], the Peng–Robinson equation of state implemented into Aspen 2006 plus software has been then used to predict the CO_2 solubility in the eight solvents without further modification. Indeed for each component, all properties required like the critical properties, T_c, P_c and V_c, normal boiling temperature, T_b, and acentric factor, ω, were already available within the Aspen databank. These calculations were performed within Aspen Plus by the simulation of a flash separator, with a mixed feed stream of selected solvent and gas, and two exit streams, one for the liquid phase and the other for the gaseous phase. The feed stream contained a large excess of gas to ensure that the limit of solubility was reached. Simulations were performed for each gas/solvent system under exactly the same conditions of temperature and pressure that were used in generating each experimental gas solubility data point. Each predicted value was determined from the simulation results as the mol fraction of gas in the liquid stream exiting the flash separator.

3. Results and discussion

3.1. Experimental data

The experimental carbon dioxide solubility values in the eight selected solvents are listed in table 2, where the solubility data are reported in terms of their CO_2 mole fractions and Henry's law constants at atmospheric pressure. For each solvent studied, experimental data points were obtained within the temperature interval between (283 and 333) K, excepted in the case of the PC, DEC and DMC, where measurements were performed up to 353 K.

To represent the CO_2 solubility in selected solvents as a function of temperature, experimental data were then correlated over the whole temperature range by using the following empirical equation:

$$\ln\left(\frac{K_H(T)}{p^0}\right) = \sum_{i=0}^{n} A_i (T/K)^{-i}. \tag{4}$$

The coefficients A_i obtained in the fit are reported in table 3 together with the relative absolute average deviation, RAAD obtained for each solute calculated as:

TABLE 2

Experimental values of CO_2 solubility in selected solvents expressed both as Henry's law constants, K_H and as CO_2 mole fraction, x_2, at atmospheric pressure. δ are relative deviations calculated from each correlation reported in table 3.

Solvent	T/K	$10^2 \cdot x_{CO2}{}^a$	K_H/MPa^a	$100 \cdot \delta$
EC	291.15	0.622^b	16.08^b	0.17
	298.15	0.573^c	17.44^c	−0.70
	313.15	0.489^b	20.47^b	1.21
	333.15	0.364^b	27.51^b	−1.02
	353.15	0.274	36.51	0.35
PC	283.15	1.496	6.69	−0.60
	298.15	1.088	9.19	0.94
	316.15	0.766^b	13.06^b	−1.01
	333.15	0.598	16.72	0.42
	353.15	0.461	21.70	−0.02
γBL	283.15	1.167	8.57	−0.58
	298.15	0.862	11.60	1.40
	313.15	0.635	15.74	−0.55
	333.15	0.454	22.01	−0.67
	353.15	0.344	29.09	0.43
DMC	283.15	1.946	5.14	−0.24
	298.15	1.361	7.35	0.88
	316.15	0.913^b	10.95^b	−1.31
	333.15	0.690	14.50	0.89
	353.15	0.504	19.83	−0.20
EMC	283.15	2.263	4.42	−0.48
	298.15	1.696	5.90	−0.86
	313.15	1.385	7.22	4.89
	333.15	0.912	10.97	−5.65
	353.15	0.745	13.42	2.03
DEC	283.15	2.128	4.70	−0.09
	298.15	1.652	6.05	0.28
	316.15	1.252	7.99	−0.30
	333.15	1.002	9.98	0.13
	353.15	0.790	12.66	−0.01
MP	283.15	3.070	3.26	0.11
	298.15	2.140	4.67	−0.36
	313.15	1.536	6.51	0.35
	333.15	1.001	9.99	−0.10
EA	283.15	2.864	3.49	0.18
	298.15	1.977	5.06	−0.59
	313.15	1.490	6.71	0.57
	333.15	1.086	9.21	−0.17

[a] Precision and accuracy of the reported experimental data are close to (1 and 15)%, respectively.
[b] Experiment data from Blanchard et al. [18].
[c] Measured in its sub-cooled liquid state after heating at $T = 353$ K.

$$RAAD = \frac{1}{N}\left|\frac{Y_{exptl} - Y_{calcd}}{Y_{calcd}}\right| = \frac{1}{N}|\delta| \qquad (5)$$

where N is the total number of data points, Y_{exptl} and Y_{calcd} are the experimental and calculated data for the studied property, respectively. The δ is the relative deviation between experimental and calculated data. According to Jacquemin et al. [50] the precision of the experimental results can be evaluated from these deviations, which is herein less than 1% except in the case of the CO_2 solubility in MP.

Figure 3 represents the CO_2 solubility data, expressed in mole fraction of CO_2 (a) as well as in Henry's Law constants (b) at the atmospheric pressure, in the selected pure solvents as a function of temperature. It can be observed that the CO_2 is more soluble in linear solvents than in cyclic carbonates, as already described in the literature by our group [18] and others [23,33].

These reported CO_2 solubility data can be also compared with those reported in the literature by our group previously [18] as well as by others [19–33]. From table 4 and figure 4, it can be seen that the values of CO_2 solubility in PC are in excellent agreement with published data by Blanchard et al. [18], Issacs et al. [20], Zubchenko et al. [21], Xu et al. [27] and Schmack and Bittrich [28] within a per cent RAAD close to (1.8, 3.2, 8.7, 8.5, and 7.9)%,

TABLE 3

Parameters of equation (4) used to smooth the experimental CO_2 solubility results from table 2 along with the relative average absolute deviation of the fit (*RAAD*).

Solvent	A_0	A_1	A_2	$100 \cdot RAAD$
EC	+18.364	$-6.9045 \cdot 10^3$	$+8.8437 \cdot 10^5$	0.7
PC	+6.811	$+4.4136 \cdot 10^2$	$-3.3434 \cdot 10^5$	0.6
γBL	+9.610	$-1.0909 \cdot 10^4$	$-1.0519 \cdot 10^5$	0.7
DMC	+7.949	$-1.4601 \cdot 10^2$	$-2.8029 \cdot 10^5$	0.7
EMC	+9.960	$-1.9034 \cdot 10^3$	$+4.3759 \cdot 10^4$	2.8
DEC	+8.323	$-1.0803 \cdot 10^3$	$-5.2814 \cdot 10^4$	0.2
MP	+14.083	$-4.0502 \cdot 10^3$	$+2.9706 \cdot 10^5$	0.2
EA	+3.413	$+2.2322 \cdot 10^3$	$-6.2072 \cdot 10^5$	0.4

respectively. Nevertheless, higher deviations were found with the published data of Murrieta-Guevara et al. [25,26] (14%), Mantor et al. [19] (16%), Rivas and Prausnitz [22] (14%), Hongling et al. [23] (20%), and Lenoir et al. [24] (up to 30%). Even if the origin of such differences is difficult to understand clearly, such deviations could come from the difference of experimental techniques used by each group, the solvent-purity and water content in each sample. From this comparison, it seems clear that the uncertainty of reported solubility data herein and in the literature is close to 15% in each case. Nevertheless, it appears also that our previous values should be considered in relation to the present ones with accuracy close to 2%. Finally, to date, to the best of our knowledge, there was no value of CO_2 solubility in EMC and MP reported in the literature.

From table 2 and figure 3, it can be appreciated that at $T = 298$ K the CO_2 solubility increases in the following order: EC < γBL < PC < DMC < DEC < EMC < EA < MP. For each solvent, the CO_2 solubility decreases with temperature, for example the CO_2 solubility in PC and DEC are close to (0.011 and 0.016) and to (0.006 and 0.010) in CO_2 mole fraction units at $T = (298$ and $333)$ K and atmospheric pressure, respectively. Nevertheless, depending on the selected solvent, different CO_2 solubility variations with the temperature are found. At $T = 333$ K increase of the CO_2 solubility in the following order: EC < γBL < PC < DMC < DEC ⩽ EMC < MP < EA, is different from the ranking obtained at $T = 298$ K. Such a difference could be explained by the various solvent structures. In other words, steric effects may explain the fact that CO_2 is less soluble in cyclic carbonates than in acyclic solvents. Generally, in both homologous series of solvents reported by our group herein and previously – i.e. cyclic and acyclic carbonates, lactones – the CO_2 solubility increases with the molar mass of the solvent [18]. Nevertheless, as the CO_2 solubility is higher in EMC than in DEC, the variation of the CO_2 solubility does not follow exactly the variation of their molar masses. In this case, the linear carbonate solvent with a non-symmetric structure has higher CO_2 solubility than that with a symmetric structure. This is confirmed by the fact that CO_2 presents higher solubility values in EA and MP solvents than those reported with linear carbonates. The difference obtained for the CO_2 solubility in each studied solvent as a function of temperature may be due to the fact that their solubility is driven by different dissolution pathways, which can be governed by the CO_2–solvents interactions, as well as by the reorganization of the solvent in the presence of CO_2.

3.2. Solvation properties

From the knowledge of the variation of the CO_2 solubility in solvents as a function of temperature, expressed in Henry's law constant, it is then possible to calculate their dissolution properties like the standard Gibbs energy, enthalpy and entropy of the dissolution of the CO_2 in studied solvents [51]:

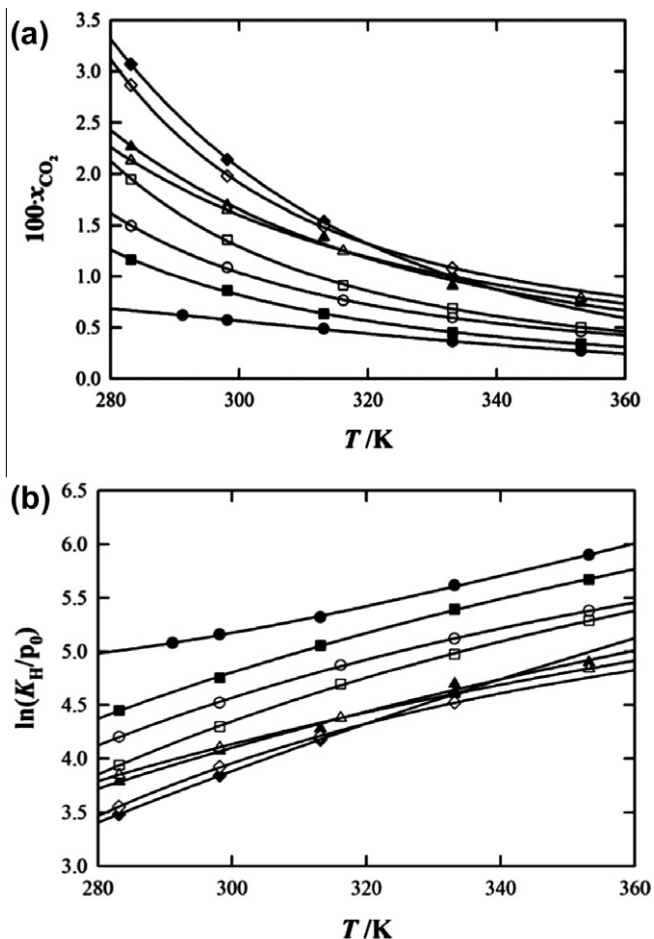$$\Delta_{dis}G^0 = RT \ln\left(\frac{K_H}{p^0}\right), \qquad (6)$$

FIGURE 3. CO_2 solubility as a function of temperature in: •, EC; ○, PC; ■, γBL; □, DMC; ▲, EMC; △, DEC; ♦ MP; ◇, EA expressed: (a) as CO_2 mole fraction and (b) as $\ln(K_H)$. Lines represent the smoothed data using the parameters in table 3.

$$\Delta_{dis}H^0 = -T^2 \partial/\partial T \left(\frac{\Delta_{dis}G^0}{T} \right) = -RT^2 \partial/\partial T \left[\ln\left(\frac{K_H}{p^0} \right) \right], \quad (7)$$

$$\Delta_{dis}S^0 = \frac{(\Delta_{dis}H^0 - \Delta_{dis}G^0)}{T}, \quad (8)$$

where p° is the standard state pressure.

The CO_2 dissolution in solvents can be viewed as a two-step process involving an intermediate step, in which the CO_2 is considered in its hypothetical liquid state driven by its standard enthalpy of liquefaction, $\Delta_{liq}H^\circ$, as schematized in figure 5 [18,51].

In other words, the enthalpy of mixing of the CO_2 with solvent, $\Delta_{mix}H^\circ$, can be calculated as:

$$\Delta_{dis}H^0 = \Delta_{liq}H^0 + \Delta_{mix}H^\circ, \quad (9)$$

where $\Delta_{liq}H^\circ = -16.90 \text{ kJ} \cdot \text{mol}^{-1}$ at $T = 298.15$ K [51].

The values for the standard Gibbs energy, enthalpy and entropy of dissolution of the CO_2 in the eight solvents are given in table 5, as well as their enthalpies of mixing. As expected, the standard Gibbs energies of dissolution of CO_2 in solvents are positive, and follow the same order as that reported for the solubility, since the Gibbs energy is directly proportional to the logarithm of the Henry's law constants. The standard enthalpies and entropies of dissolution of CO_2 in solvents are all negative. In other words the CO_2 solubility in each solvent is entropy-driven and presents an exothermic process of dissolution. From table 5, it can be seen also that all enthalpies of mixing are positive except in the case of the

TABLE 4

Literature values of CO_2 solubility in selected solvents expressed both as Henry's law constants, K_H and as CO_2 mole fraction, x_2, at atmospheric pressure. The values of δ are relative deviations calculated between literature values and those calculated from each correlation reported in table 3.

Solvent	T/K	$10^2 \cdot x_{CO_2}$	K_H/MPa	$100 \cdot \delta$	Reference
PC	275	1.876	5.33	−1.88	[18]
	291	1.206	8.29	3.90	
	298.15	1.079	9.27	−0.08	
	316	0.766	13.06	1.28	
	298.15	1.233	8.113	−12.55	[19]
	299.85	1.224	8.17	−14.89	
	310.95	0.983	10.17	−13.97	
	313.15	0.966	10.35	−15.75	
	323.15	0.828	12.08	−16.55	
	344.25	0.627	15.94	−18.16	
	348.15	0.589	16.98	−16.94	
	373.15	0.450	22.23	−17.18	
	377.15	0.439	22.78	−18.31	
	313.15	0.858	11.65	−5.16	[20]
	373.15	0.377	26.5	−1.28	
	313.15	0.887	11.27	−8.26	[21]
	343.15	0.602	16.6	−13.57	
	373.15	0.389	25.73	−4.14	
	298.15	1.208	8.28	−10.75	[22]
	323.15	0.812	12.31	−14.96	
	373.15	0.453	22.06	−17.82	
	313	1.007	9.93	−18.96	[23]
	333	0.803	12.46	−25.63	
	353	0.588	17.02	−21.43	
	373	0.442	22.65	−15.50	
	298.15	1.477	6.77	−27.03	[24]
	323.15	0.971	10.3	−28.85	
	343.15	0.806	12.4	−35.44	
	298.15	1.218	8.21	−11.50	[26]
	313.15	0.978	10.23	−16.72	
	373.15	0.346	28.88	7.59	
	298.15	1.269	7.88	−15.06	[25]
	323.15	0.857	11.67	−19.38	
	298	1.190	8.4	−9.18	[27]
	303	1.053	9.5	−6.95	
	313	0.855	11.7	−4.51	
	323	0.800	12.5	−13.45	
	298.15	0.999	10.01	7.90	[28]
$100 \cdot RAAD$				13.5	[18–28]
γBL	275	1.393	7.18	2.23	[18]
	291	1.015	9.85	−2.83	
	298.15	0.859	11.64	−1.04	
	316	0.606	16.5	0.19	
	303	1.580	6.33	−51.12	[29]
$100 \cdot RAAD$				11.5	[18,29]
DMC	283	1.848	5.41	5.93	[18]
	291	1.621	6.17	−1.48	
	298.15	1.337	7.48	0.88	
	316	0.913	10.95	1.62	
	280.7	2.442	4.0958	−14.69	[30]
	289.49	1.985	5.0377	−16.51	
	298.47	1.593	6.2758	−15.97	
	307.84	1.342	7.4536	−18.58	
	317.86	1.159	8.6316	−22.69	
	327.66	1.014	9.8571	−26.05	
$100 \cdot RAAD$				12.4	[18,30]
DEC	275	2.469	4.05	0.49	[18]
	291	1.855	5.39	0.00	
	298.15	1.647	6.07	0.03	
	316	1.252	7.99	0.52	
EC	291	0.622	16.08	−0.03	[18]
	298.15	0.573	17.46	0.80	
	313	0.489	20.47	−1.00	
	333	0.364	27.51	1.25	
	313	0.694	14.41	−30.31	[31]
$100 \cdot RAAD$				6.7	[18,31]
EA	298.15	2.299	4.35	−13.48	[32]

dissolution of the CO_2 in MP, which confirm our previous results [18] and clearly indicate the lack of specific interaction between
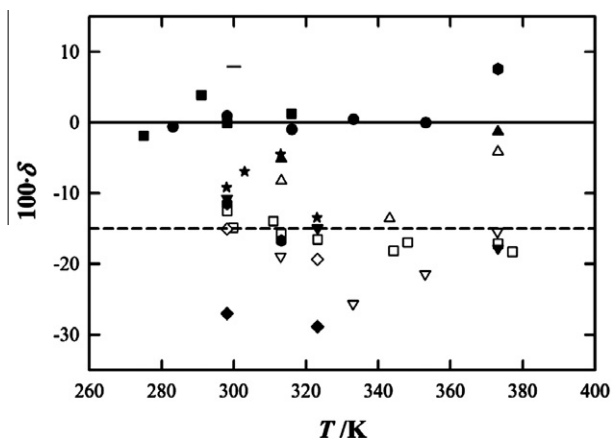
FIGURE 4. Relative deviations, δ, of CO_2 solubility in PC between data presented in the present work with those from the literature: •, this work; ■, Blanchard et al. [18]; □, Mantor et al. [19]; ▲, Issacs et al. [20]; △, Zubchenko et al. [21]; ▽, Rivas and Prausnitz [22]; ▼, Hongling et al. [23]; ♦, Lenoir et al. [24]; ◇, Murrieta-Guevara et al. [25]; ●, Murrieta-Guevara et al. [26]; ★, Xu et al. [27]; –, Schmack and Bittrich [28].
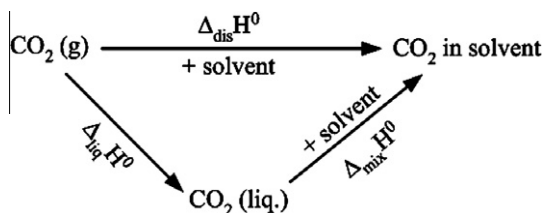

FIGURE 5. Thermodynamic pathway of the CO_2 dissolution in solvents.

selected solvents and CO_2. The difference observed between mixing enthalpies of CO_2 with EA and with MP, reinforces the hypothesis that these solvents are probably driven by different molecular mechanisms of dissolution.

3.3. Calculated data

In order to evaluate different tools able to predict the gas solubility in pure electrolyte–solvent, experimental results presented herein were then compared with those calculated by COSMOthermX and by the Peng–Robinson equation of State implemented within Aspen 2006 plus.

Henry's law constants can be determined directly (Henry's law option) or indirectly (gas solubility option) using the COSMOthermX program. In each method, the partial vapour pressure, and thus gas solubility, is estimated using the following equation:

$$p_{(i)} = p_o^{vap}(i)x_{(i)}\gamma_{(i)}, \tag{10}$$

where $p_{(i)}, p_o^{vap}(i), x_{(i)}, g_{(i)}$ are the partial and pure vapour pressures, mole fraction and activity coefficient of a selected gaseous species i in a particular solvent.

This equation shows that for such predictions the calculation of the pure species vapour pressure and the activity coefficient are required. As reported by Ab Manan et al. [39] COSMOThermX has two main options for estimation/evaluation of the vapour pressure. The first method uses the following equation for the gas phase chemical potential, which is related to the vapour pressure;

$$\mu_{Gas}^{X_i} = E_{Gas}^{X_i} + E_{COSMO}^{X_i} - E_{vDw}^{X_i} + \omega_{Ring}n_{Ring}^{X_i} + \eta_{Gas}RT \tag{11}$$

with, $E_{Gas}^{X_i}$, $E_{COSMO}^{X_i}$ and $E_{vDw}^{X_i}$ are the quantum chemical total energies of the molecule in the gas phase, the COSMO conductor, and the van der Waals energy of species X_i, respectively. The other terms relate to a correction term for ring shaped molecules with $n_{Ring}^{X_i}$ being the number of ring atoms in the molecule and ω_{Ring} being an adjustable parameter physically predetermined by Cosmologic, as well as η_{Gas} which is a link between the reference states of the system's free energy in the gas and liquid phase [38].

The value for $E_{Gas}^{X_i}$ can be determined using a program such as Turbomole [47], denoted herein as the 'energy value'. The second method is to employ experimental data for pure components [40–46], or the constants for standard correlations derived from such data, denoted as the 'vapour value'. Here experimental $p_o^{vap}(i)$ values of the solvents studied were recalculated using an unique semi-empirical correlation, such as the following Antoine equation:

$$\ln[p_0^{vap}/kPa] = A + \frac{B}{T+C}, \tag{12}$$

where A, B and C are empirical parameters reported in table 6, calculated from vapour pressure (p_0^{vap}/kPa) experimental data as a function of the temperature (T/K) from the literature [41–46].

The comparison of predicted vapour pressures using the 'energy values' with those correlated with the 'vapour values' from equation (12) and parameters reported in table 6 implemented into COSMOthermX for each solvent as a function of the temperature is presented in table S1 of the supporting information and illustrated in figure 6. From this work, it appears that vapour pressures using the 'energy values' are underestimated except in the case of the EC where a relative deviation up to 7% is observed at T = 353 K, as well as in the case of the γBL with a RAAD close to 5% over the whole temperature range covered in this work. A RAAD close to 40% was calculated between vapour pressures estimated by COSMOthermX using 'energy values' in comparison with those from the 'vapour values'. Nevertheless, as viewed in figure 6, COSMOthermX is able to predict qualitatively the correct volatility trend as a function of the chemical structure of involved solvents, even if COSMOthermX predicts by using 'energy values' wrongly a highest volatility of the MP (8.17 kPa at T = 298 K) in comparison with the EA (5.22 kPa at T = 298 K). In order to analyse in greater detail the phase behaviour predictive capability of COSMOthermX for

TABLE 5
Thermodynamic parameters and CO_2 solubility expressed in Henry's law constant for studied solvents at T = 298 .

Solvent	M/(g · mol^{-1})	T_{vap} [40]/K	K_H^a/MPa	$\Delta_{dis}G^{\circ a}$/kJ · mol^{-1}	$\Delta_{dis}H^{\circ a}$/(kJ · mol^{-1})	$\Delta_{mix}H^{\circ a}$/(kJ · mol^{-1})	$\Delta_{dis}S^{\circ a}$/(J · K^{-1} · mol^{-1})
EC	88.06	516.7	17.44	12.78	−8.08	8.82	−69.96
PC	102.08	513.2	9.19	11.23	−14.98	1.92	−87.90
γBL	86.09	479.2	11.60	11.82	−14.94	1.96	−89.73
DMC	90.08	363.5	7.35	10.67	−16.85	0.05	−92.30
EMC	104.10	381.3 [42]	5.90	10.08	−13.38	3.52	−78.71
DEC	118.13	399.6	6.05	10.18	−11.93	4.97	−74.14
MP	86.09	353.0	4.67	9.52	−17.11	−0.21	−89.31
EA	86.09	350.2	5.06	9.71	−16.06	0.84	−86.43

^{a} Accuracy of the reported data are close to 15%.

TABLE 6
Antoine coefficients calculated from equation (12).

Solvent	A	B/K	C/K	Calculated from
EC	14.9431	4228.86	−102.23	[44]
PC	15.2569	4796.88	−63.99	[43]
γBL	15.6071	4894.55	−32.72	[41,43]
DMC	14.8144	3253.55	−44.25	[42]
EMC	14.8075	3376.60	−49.46	[42]
DEC	13.5461	2817.83	−84.30	[42]
MP	15.1621	3275.09	−40.61	[45]
EA	14.2484	2819.91	−57.44	[46]

studied solvents, data from Fang et al. [44] in the case of the (vapour + liquid) equilibrium of (DMC + EC) binary mixture were then compared with those predicted by COSMOthermX as reported in figure 7. From this figure, it appears that COSMOthermX is able to predict the phase behaviour and vapour pressures of binary mixture of (DMC + EC) within a good accuracy up to 13%. In other words, COSMOthermX software can be used to predict the vapour pressure of pure solvents and binary mixtures of electrolyte solvents for lithium ion batteries within a good predictability, which is required during the CO_2 solubility calculations, and such information can be also directly linked to the security of lithium ion batteries designs.

In the light of this vapour pressure analysis, the CO_2 solubility in solvents was then calculated by using COSMOthermX as well as the Peng–Robinson equation of state, denoted EoS-PR, implemented into Aspen 2006 plus, and are then compared, in table 7, with experimental data measured in this work at the arbitral temperature of 298 K. From this work, it appears that both methods are able to predict the CO_2 solubility in solvents within accuracy up to (36 and 24)% for COSMOthermX and Peng–Robinson equation of state implemented in Aspen Plus 2006, respectively. However, both methodologies seem to be unable to predict the CO_2 solubility order observed experimentally - for examples, both methods predict higher CO_2 solubility in γBL than in PC, as well as lower CO_2 solubility in MP (or EA) than in DEC. However, in each case, the CO_2 solubility in solvents is calculated with the respect of the order of magnitude giving in fact the possibility to use these tools for CO_2 solubility screening prior to experimental measurements. Additionally, a preliminary evaluation of the CO_2 solubility prediction in different binary mixtures like (DMC + EC), (DMC + PC) and (DMC + DEC) using COSMOThermX and Aspen 2006 has been then realised and reported in table 7. From which, it appears that both methodologies are able to predict not only the order of magnitude of the reported CO_2 solubility in these binary mixtures but also the CO_2 solubility order described into the literature [33].

To evaluate the CO_2 capture capacity of these solvents in comparison with other solvent classes generally classified for such applications like the ionic liquids [35], their Henry's law constants were compared as illustrated in figure 8. From this figure, it appears that the MP and EA solvents have comparable CO_2 solubility to those reported with the classical ionic liquids like [C_4mim][BF_4] [50], and [C_4mim][PF_6] [52], but lower than those reported with the [$C_n$mim][NTf$_2$] series [53]. This result confirms the hypothesis to use these solvents for the CO_2-capture, as already claimed by different research groups [23,30]. Furthermore, COSMOThermX calculations were performed to evaluate the effect additives such as LiPF$_6$, or [C_2mim][NTf$_2$] ionic liquid, on the CO_2 solubility in MP at T = 298 K, as reported in figure 9. From this work, it appears that the addition of lithium decreases the CO_2 solubility in MP, a contrario of the addition of the ionic liquid, which increases the CO_2 solubility in MP in comparison with the value reported in the pure solvent. Furthermore, the addition of salt in MP has the advantage to decrease the vapour pressure of the solution in comparison with the vapour pressure of pure MP. For example, at
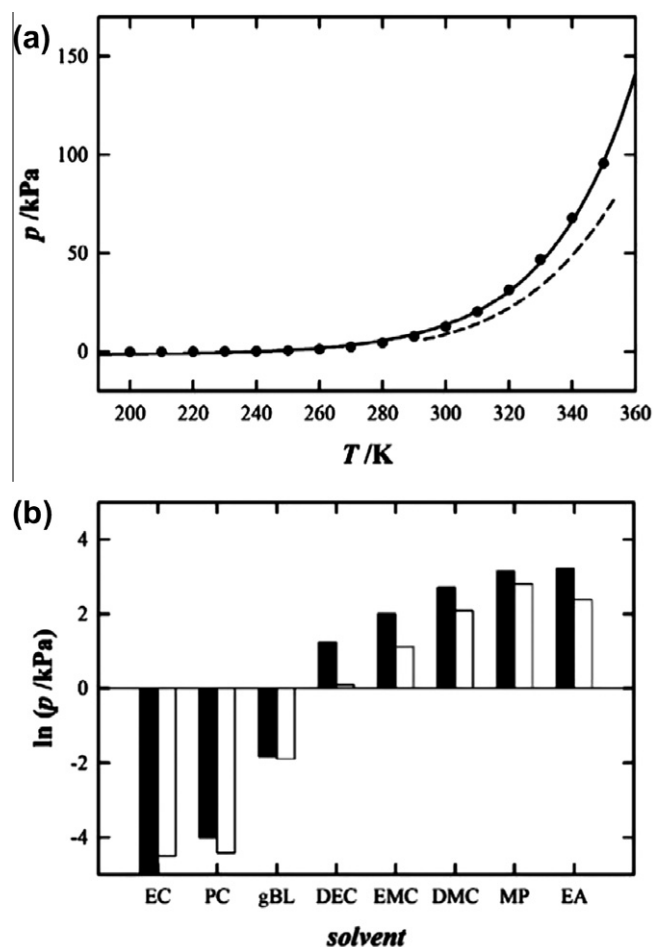

FIGURE 6. COSMOthermX calculations of vapour pressures: a) in the case of MP as a function of temperature by using: •, 'vapour value'; dashed line, 'energy value'; b) for all selected solvents at T = 298 K using: black bars, 'vapour values'; white bars, 'energy values'.
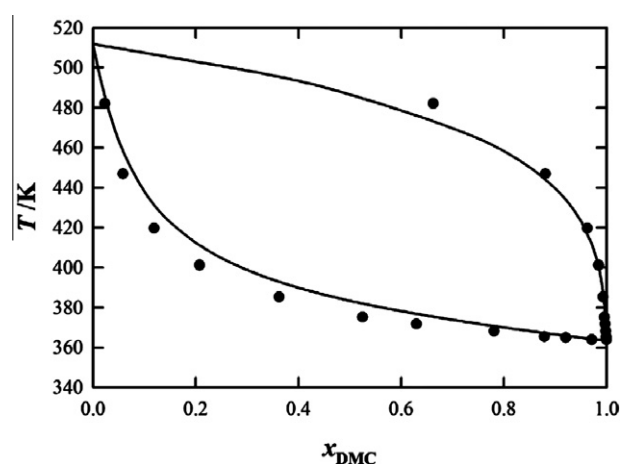

FIGURE 7. COSMOthermX calculations of the VLE of the (DMC + EC) at 101.325 kPa as a function of the DMC mole fraction vapour pressures. •, experimental data from Fang et al. [44]; solid line, calculated from COSMOthermX.

T = 298 K, COSMOthermX predicts that salt additions up to 3 M of LiPF$_6$ or of [C_2mim][NTf$_2$] decrease the MP vapour pressure up to (28.4 or 27.3)%, respectively. In other words, a salting-out and a salting-in effects are observed for the CO_2 solubility in MP by adding lithium salt and ionic liquid, respectively. This result could

TABLE 7
Comparisons of CO_2 solubility in solvents between experimental data with those calculated by COSMOthermX and by the Peng–Robinson equation of state, EoS-PR implemented in Aspen 2006 Plus at $T = 298$ K at atmospheric pressure. For each reported binary mixture, according to the experimental values reported by Gui *et al.* [33], a volume ratio of (1:1) has been used during all calculations.

Solvent	Experimental – this work[a]		COSMOThermX		EoS-PR	
	$10^2 \cdot x_{CO2}$	K_H/MPa	$10^2 \cdot x_{CO2}$	K_H/MPa	$10^2 \cdot x_{CO2}$	K_H/MPa
EC	0.57	17.44	0.53	18.78	0.80	12.45
PC	1.09	9.19	0.87	11.49	1.24	8.06
γBL	0.86	11.6	1.18	8.46	1.26	7.95
DMC	1.36	7.35	2.16	4.62	1.90	5.25
EMC	1.70	5.90	2.40	4.16	2.14	4.17
DEC	1.65	6.05	2.57	3.89	2.17	4.62
MP	1.98	5.05	2.40	4.16	1.95	5.12
EA	2.14	4.67	2.47	4.05	1.96	5.11
DMC+EC	1.04 [33]	9.66 [33]	1.66	6.03	0.93	10.81
DMC+PC	1.28 [33]	7.83 [33]	1.95	5.13	1.07	9.34
DMC+DEC	1.74 [33]	5.75 [33]	2.32	4.30	2.25	4.44

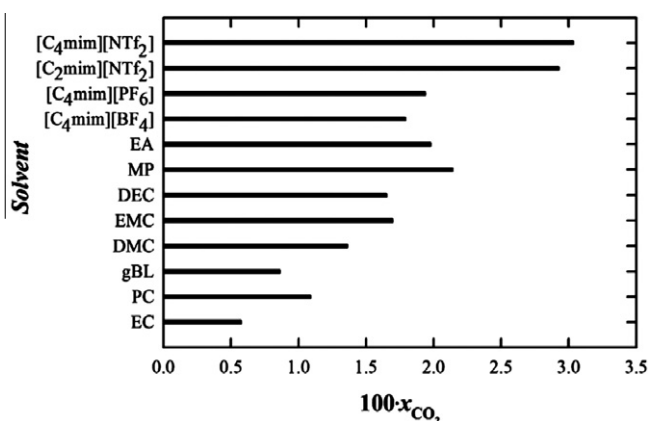[a] Precision and accuracy of the reported experimental data are close to (1 and 15)%, respectively.

FIGURE 8. Comparison between CO_2 solubility, expressed as CO_2 mole fraction, in selected solvents and in ionic liquids: [C4mim][BF4] [50], [C4mim][PF6] [52], [C2mim][NTf2] [53], and [C4mim][NTf2] [53] at $T = 298$ K and atmospheric pressure.
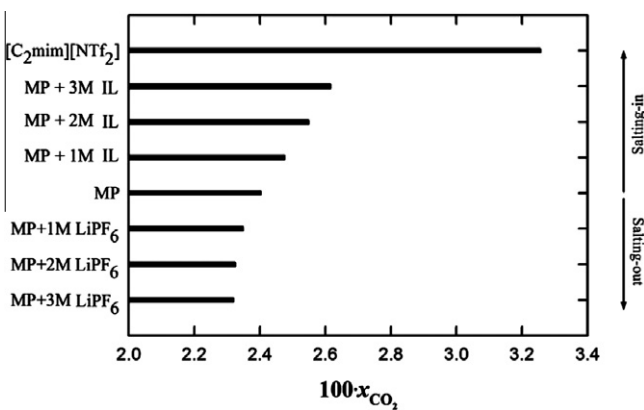

FIGURE 9. Effect of the addition of a salt like a lithium salt: LiPF6, or an ionic liquid: [C2mim][NTf2] on the CO_2 solubility in MP at $T = 298$ K and atmospheric pressure calculated by COSMOthermX.

drive other studies based on the evaluation of the gas solubility in binary mixtures containing an ionic liquid mixed with a pure-electrolyte solvent, but not only focused on Li-ion battery applications.

4. Conclusions

We report the CO_2 solubility in eight different pure electrolyte solvents for lithium ion batteries such as ethylene carbonate, propylene carbonate, dimethyl carbonate, ethyl methyl carbonate, diethyl carbonate, γ-butyrolactone, ethyl acetate and methyl propionate as a function of temperature at atmospheric pressure. The results could be compared with literature data and the experimental technique could be validated with precision and accuracy close to ±(1 and 15)%, respectively. The CO_2 solubility in solvents varies significantly over the temperature range covered and it appears that the CO_2 is more soluble in acyclic than in cyclic solvents. Furthermore, it was also observed that the CO_2 is more soluble in linear carbonate solvent presenting a non-symmetric structure. As expected, the CO_2 solubility in all solvents decreases with temperature and the dissolution of the CO_2 in all solvents is entropy-driven and exothermic. The data obtained make it possible also to calculate the mixing enthalpy of (CO_2 + solvent) mixtures in its hypothetical liquid state, which can provide information for molecular interactions in solution. All enthalpies of mixing are positive except in the case of the dissolution of the CO_2 in MP, which clearly indicate the lack of specific interaction between selected solvents and CO_2. Furthermore, the difference observed between mixing enthalpies of CO_2 with EA and with MP, reinforces the hypothesis that these solvents are probably driven by different molecular mechanisms of dissolution. Finally, CO_2 solubility was then predicted using COSMOthermX and the Peng–Robinson equation of state implemented in Aspen 2006 Plus with accuracies close to (36 and 24)%, respectively. These results confirm that these tools could be used to screen, prior experimental measurements, the solubility of species in pure-electrolyte solvent for Li-ion batteries in that way salting-out and salting-in effects were observed in the case of the CO_2 solubility in MP by adding a lithium salt and an ionic liquid, respectively. These salting effects have been experimentally investigated in different binary and ternary mixtures by our group and will be and will be presented and discussed in later publications.

Appendix A. Supplementary data

Supplementary data associated with this article can be found, in the online version, at doi:10.1016/j.jct.2012.01.027.

Additional Supporting Information includes calculated vapour pressure of pure molecular solvents as a function of temperature, used as a comparison with the experimental values calculated from equation (12) with parameters reported in table 6. This material is available free of charge via the Internet.

References

[1] R. Korhonen, K. Pingoud, I. Savolainen, R. Matthews, Environ. Sci. Policy 5 (2002) 429–441.
[2] S. Amjad, S. Neelakrishnan, R. Rudramoorthy, Renew. Sust. Energ. Rev. 14 (2010) 1104–1110.
[3] J.M. Tarascon, M. Armand, Nature 414 (2001) 359–367.
[4] D. Aurbach, E. Zinigrad, Y. Cohen, H. Teller, Solid State Ionics 148 (2002) 405–416.
[5] M.Q. Xu, L.D. Xing, W.S. Li, X.X. Zuo, D. Shu, G.L. Li, J. Power Sources 184 (2008) 427–431.
[6] H.L. Zhang, C.H. Sun, F. Li, C. Liu, J. Tan, H.M. Cheng, J. Phys. Chem. C 111 (2007) 4740–4748.
[7] B. Scrosati, J. Hassoun, Y.K. Sun, Energy Environ. Sci. 4 (2011) 3287–3295.
[8] B. Scrosati, J. Garche, J. Power Sources 195 (2010) 2419–2430.
[9] M.C. Smart, B.V. Ratnakumar, K.B. Chin, L.D. Whitcanack, J. Electrochem. Soc. 157 (2010) A1361–A1374.
[10] M.C. Smart, B.V. Ratnakumar, L.D. Whicanack, K.A. Smith, S. Santee, F.J. Puglia, R. Gitzendanner, ECS Trans. 25 (2010) 273–282.
[11] M. Ue, A. Murakami, S. Nakamura, J. Electrochem. Soc. 149 (2002) A1572–A1577.
[12] M. Arakawa, J.-I. Yamaki, J. Power Sources 54 (1995) 250–254.
[13] M. Ue, M. Takeda, M. Takehara, S. Mori, J. Electrochem. Soc. 144 (1997) 2684–2688.
[14] S.A. Freunberger, Y. Chen, Z. Peng, J.M. Griffin, L.J. Hardwick, F. Bardé, P. Novak, P.G. Bruce, J. Am. Chem. Soc. 133 (2011) 8040–8047.
[15] S.A. Freunberger, Y. Chen, N.E. Drewett, L.J. Hardwick, F. Bardé, P.G. Bruce, Angew. Chem. 50 (2011) 8609–8613.
[16] M. Moshkovich, M.J. Cojocaru, H.E. Gottlieb, D. Aurbach, J. Electroanal. Chem. 497 (2001) 84–96.
[17] F. Joho, P. Novak, Electrochim. Acta 45 (2000) 3589–3599.
[18] F. Blanchard, B. Carré, F. Bonhomme, P. Biensan, D. Lemordant, Can. J. Chem. 81 (2003) 385–391.
[19] P.D. Mantor, O. Abib, K.Y. Song, R. Kobayashi, J. Chem. Eng. Data 27 (1982) 243–245.
[20] E.E. Issac, F.D. Otto, A.E. Mather, Can. Chem. Eng. J. 55 (1977) 751–752.
[21] Y.P. Zubchenko, S.F. Shakhova, T. Wei, L.I. Titelman, L.K. Kaplan, Zh. Prikl. Khim. 44 (1971) 2044–2047.
[22] O.R. Rivas, J.M. Prausnitz, AIChE J. 25 (1979) 975–984.
[23] L. Hongling, Z. Rongjiao, X. Wei, L. Yanfen, S. Yongju, T. Yiling, J. Chem. Eng. Data 56 (2011) 1148–1157.
[24] J.Y. Lenoir, P. Renault, H. Renon, J. Chem. Eng. Data 16 (1971) 340–342.
[25] F. Murrieta-Guevara, A.T. Rodriguez, J. Chem. Eng. Data 29 (1984) 456–460.
[26] F. Murrieta-Guevara, A.R. Martinez, A.T. Rodriguez, Fluid Phase Equilib. 44 (1988) 105–115.
[27] Y. Xu, R.P. Schutte, L.G. Hepler, Can. Chem. Eng. J. 70 (1992) 569–573.
[28] P. Schmack, H.J. Bittrich, in: A.L. Kohl, F.C. Riesenfeld (Eds.), Gas Purification, second ed., Gulf Publishing Co., Houston, 1974. Chapter 14.
[29] D.M. Kassim, H.A. Zainel, S.A. Al-Asaf, E.K. Talib, Fluid Phase Equilib. 41 (1988) 287–294.
[30] X. Gui, Z. Tang, W. Fei, J. Chem. Eng. Data 55 (2010) 3736–3741.
[31] R. Vilcu, S.T. Perisanu, M. Cucuiat, Pol. J. Chem. 54 (1980) 2043–2050.
[32] S.T. Perisanu, J. Solution Chem. 30 (2001) 183–192.
[33] X. Gui, Z. Tang, W. Fei, Low Carbon Econ. 2 (2011) 26–31.
[34] E. Wilhelm, R. Battino, Chem. Rev. 73 (1973) 1–9.
[35] L.A. Blanchard, D. Hancu, E.J. Beckman, J.F. Brennecke, Nature 399 (1999) 28–29.
[36] H. Kim, Y. Ding, P.A. Kohl, J. Power Sources 198 (2012) 281–286.
[37] J.H. Dymond, E.B. Smith, The Virial Coefficients of Pure Gases and Mixtures, Clarendon Press, Oxford, 1980.
[38] F. Eckert, A. Klamt, COSMOtherm User's Manual: Version C2.1, Release 01.06 2006, COSMO logic GmbH & Co. KG, Leverkusen, Germany.
[39] N. Ab Manan, C. Hardacre, J. Jacquemin, D.W. Rooney, T.G.A. Youngs, J. Chem. Eng. Data 54 (2009) 2005–2022.
[40] http://webbook.nist.gov/ (accessed: 03.11.11).
[41] H.P. Luo, J.H. Zhou, W.D. Xiao, K.H. Zhu, J. Chem. Eng. Data 46 (2001) 842–845.
[42] X. Zhang, J. Zuo, C. Jian, J. Chem. Eng. Data 55 (2010) 4896–4902.
[43] T. Mathuni, J.-I. Kim, S.-J. Park, J. Chem. Eng. Data 56 (2011) 89–96.
[44] Y.-J. Fang, J.-M. Qian, J. Chem. Eng. Data 50 (2005) 340–343.
[45] C.-T. Hsieh, W.-Y. Ji, H.-m. Lin, M.-J. Lee, Fluid Phase Equilib. 271 (2008) 69–75.
[46] D. Ambrose, J.H. Ellender, H.A. Gundry, D.A. Lee, R. Townsend, J. Chem. Thermodyn. 13 (1981) 795–802.
[47] R. Ahlrichs, TURBOMOLE User's Manual: Version 5.7 2004, COSMOlogic GmbH & Co. KG, Leverkusen, Germany.
[48] C. Hardacre, J. Jacquemin, N. Ab Manan, D.W. Rooney, T.G.A. Youngs, Prediction of gas solubility using COSMOthermX, in: N.V. Plechkova, R.D. Rogers, K.R. Seddon (Eds.), ACS Symposium Series Ionic Liquids. 1030. Ionic Liquids: From Knowledge to Application, American Chemical Society Publications, Washington, DC, 2009,pp. 359–383 (Chapter 24).
[49] Aspen Plus User Models, version number: 2006 online version at http://www.support.aspentech.com (accessed 03.10.11).
[50] J. Jacquemin, M.F. Costa Gomes, P. Husson, V. Majer, J. Chem. Thermodyn. 38 (2006) 490–502.
[51] J.H. Hildebrand, J.M. Prausnitz, R.L. Scott, Regular and Related Solutions, Van Nostrand Reinhold, New York, 1970.
[52] J. Jacquemin, P. Husson, V. Majer, M.F.C. Gomes, Fluid Phase Equilib. 240 (2006) 87–95.
[53] J. Jacquemin, P. Husson, V. Majer, M.F. Costa Gomes, J. Solution Chem. 36 (2007) 967–979.

JCT-11-571